River Flow 2010 - Dittrich, Koll, Aberle & Geisenhainer (eds) - © 2010 Bundesanstalt für Wasserbau ISBN 978-3-939230-00-7

Double-average methodology applied to turbulent gravel-bed river flows

M.J. Franca
IMAR – Centre for Marine and Envir. Research & FCT – New University of Lisbon, Lisbon, Portugal

R.M.L. Ferreira & A.H. Cardoso
CEHIDRO & Instituto Superior Técnico, TULisbon, Lisbon, Portugal

U. Lemmin
LHE-ENAC, École Polytechnique Fédérale de Lausanne (EPFL), Lausanne, Switzerland

ABSTRACT: For low relative roughness, the flow near the bed is three-dimensional and spatially heterogeneous, and bed forms play a major role. To incorporate the effects of bed irregularity, upscaling above the dominant wavelength of the bed forms is needed. This can be obtained by applying spatial averaging to the RANS equations resulting in the so-called double-averaged (both in time and space) Navier-Stokes equations. When compared to the RANS equations, these equations provide additional terms, i.e. form-induced stresses. The present work presents and discusses instantaneous velocity measurements made in the Swiss river Venoge, using an Acoustic Velocity Profiler (ADVP). A 3D measuring grid with 15 profiles was defined. The riverbed, composed of coarse round gravel, presented a relative submergence of 2.94. Double-averaging is applied to velocity and to fluid stresses distributions. Three regions of the flow are identified: surface, intermediate and roughness layers. The roughness layer is below $z/h \approx 0.40$, in which the stresses distribution is determined by local effects of the bed forms. Form-induced and total normal stresses peak within the roughness layer. Form-induced normal stresses within the roughness layer are of the same order of magnitude or higher than Reynolds normal stresses.

Keywords: Turbulent flow; Gravel-bed rivers; Double-averaging methodology

1 INTRODUCTION

The present study concerns field measurements in a river made under low values of relative submergence, $h/D = 2.94$, where h is the water depth and D a grain diameter representative of the riverbed material, in the present case D_{50}. Due to the high concentration of coarse elements in the riverbed, a roughness-wake effect is formed within the inner layer of the flow (Kirkbride and Ferguson 1995, Baiamonte and Ferro 1997, Buffin-Bélanger and Roy 1998). Previous studies have shown that in these 3D flows, self-similarity of time-averaged turbulence characteristics does not exist in the so-called roughness layer, a restricted lower region of the flow (Nikora and Smart 1997, Smart 1999). Due to the random variability of the bed elevation, the flow is 3D and spatially heterogeneous within a thick inner layer. Therefore, under these conditions, additional difficulties occur when modeling practical and theoretical problems related to river flows, such as river restoration, pollution control and stable channel design.

Double-averaging methods (DAM) have allowed progress in the characterization of 3D flows over irregular boundaries. DAM are a particular form of upscaling, both in time and space. The conservation equations of turbulent flows are thus expressed for (i) time-averaged quantities, which in the case of unsteady flow are defined in a time-window smaller than the fundamental unsteady flow time-scale, and for (ii) space-averaged quantities defined in space windows larger than the characteristic wavelength of the boundary irregularities (Franca and Czernuszenko 2006).

These 3D flows are common to several geophysics fields. The formulation of the theory pertaining to DAM was developed in atmospheric boundary layer studies to describe turbulent flows within and above terrestrial canopies (Raupach *et al.* 1991, Finnigan 2000, Finnigan and Shaw 2008), in the study of hydraulically rough beds due to bed forms (Smith and McLean 1977, Gimenez-Curto and Corniero Lera 1996) and to sand-gravel roughness (Nikora *et al.* 2001, Nikora *et al.* 2007, Pokrajac *et al.* 2008, Franca *et al.* 2008, Ferreira *et al.* 2009) and in the study of hydraulic flows over and within vegetation (Lopez and Garcia 2001, White and Nepf 2008). Compared to numerous DAM laboratory experiments, there are few studies based on river field measurements (cf. Buffin-Bélanger and Roy 2005).

In this paper, we apply DAM to field velocity data obtained from 15 profiles in a gravel-bed river. DAM were applied to time-averaged velocity and stress profiles measured in a 0.40 x 0.30 m^2 area roughly in the center of a 6.30 m wide gravel-bed river. We determine double-averaged velocity profiles and double-averaged normal stresses per unit mass profiles for the three Cartesian components. Additional terms arising from the application of the MA methodology to the momentum conservation equation, i.e. form-induced stresses, are quantified.

First, the theory of double-averaging methods applied to the Navier-Stokes equations is introduced. Conditions under which the field measurements were made and details on the Acoustic Doppler Velocity Profiler are then given. Finally, the empirical results are presented and discussed.

2 THEORETICAL BACKGROUND

Reynolds-averaged Navier-Stokes equations (RANS), for 3D, isothermal, steady turbulent open-channel flows of incompressible Newtonian fluids with no solid discharge, may be expressed using the following Cartesian tensor notation (Hinze, 1975):

$$\overline{u_i}\frac{\partial \overline{u_j}}{\partial x_i} = g_j - \frac{1}{\rho}\frac{\partial \overline{p}}{\partial x_j} + \frac{\partial}{\partial x_i}\overbrace{\left(\nu\frac{\partial \overline{u_j}}{\partial x_i} - \overline{u'_j u'_i}\right)}^{\tau_{ji}/\rho} \tag{1}$$

where u = velocity, x = space variable, subscripts i and j are the 3D Cartesian directions with 1 for streamwise, 2 for spanwise and 3 for vertical, g = gravity acceleration, ρ = fluid density, p = pressure, and ν = fluid kinematic viscosity. The over-bar indicates time-averaging, and the prime denotes instantaneous fluctuations. The streamwise, spanwise and vertical directions are identified by x, y and z, and the corresponding velocities, by u, v and w. Total mean stresses per unit mass, τ_{ij}/ρ, are divided into viscous and turbulent or Reynolds stresses; these are the left and right terms within the brackets, respectively.

Within the double-averaging framework we apply, to any instantaneous variable θ, a decomposition similar to the Reynolds decomposition where the spatial variability is accounted for,

$$\theta = \left\langle\overline{\theta}\right\rangle + \underbrace{\tilde{\overline{\theta}}}_{\tilde{\theta}} + \underbrace{\left\langle\theta\right\rangle' + \tilde{\theta}'}_{\theta'} \tag{2}$$

where < > is the double-averaging operator, both in time and space, and ˜ is spatial variation. Any instantaneous quantity θ is thus decomposed into a double-averaged component ($\left\langle\overline{\theta}\right\rangle$), a component corresponding to the spatial deviation from the time-averaged quantity ($\tilde{\overline{\theta}} = \overline{\theta} - \left\langle\overline{\theta}\right\rangle$), and an instantaneous component (θ').

The definition of the double-averaging operator applied to a quantity θ, over a specific horizontal plane at level z is (Nikora *et al.*, 2001),

$$\left\langle\overline{\theta}\right\rangle(z) = \frac{1}{A_f(z)}\int_{\Omega}\overline{\theta}(\alpha,\beta,z)\mathrm{d}S \tag{3}$$

Where A_f = void function corresponding to the fraction of the area occupied by the fluid at a given elevation (z) and Ω = horizontal domain located at a given elevation (z) parallel to the riverbed. The integration is made over a horizontal surface (dS). Dummy variables α and β are defined as $0 < \alpha < L_x$ and $0 < \beta < L_y$, where L_x and L_y are the streamwise and spanwise extension of the area defined by Ω. Both L_x and L_y should be larger than the wavelengths of the spatial distributions of the variations of the near-bed longitudinal velocities (Smith and McLean 1977).

For steady flows, manipulation of RANS after the application of the double-averaging operator to the time varying quantities and to the partial derivatives (cf. Nikora *et al.* 2007 on the application of DA to the derivatives) renders the DANS (Double Averaged Navier-Stokes equations),

$$\begin{aligned}\left\langle\overline{u_i}\right\rangle\frac{\partial\left\langle\overline{u_j}\right\rangle}{\partial x_i} &= g_j - \frac{1}{\Psi\rho}\frac{\partial\left(\Psi\left\langle\overline{p}\right\rangle\right)}{\partial x_j} + \\ &+ \frac{1}{\Psi}\frac{\partial}{\partial x_i}\overbrace{\left(\Psi\left\langle\nu\frac{\partial\overline{u_j}}{\partial x_i}\right\rangle - \Psi\left\langle\overline{u'_j u'_i}\right\rangle - \Psi\left\langle\tilde{u}_j\tilde{u}_i\right\rangle\right)}^{\left\langle\tau_{ji}\right\rangle/\rho} + \\ &+ f_{Dj} - f_{Vj}\end{aligned} \tag{4}$$

where f_D = pressure drag per unit mass, f_V = viscous drag per unit mass and Ψ = ratio between area occupied by the fluid (A_f) and total area for a given z.

When compared to RANS, three additional terms appear in the momentum equation: the third term within the brackets containing the total stress tensor, corresponds to the form-induced or dispersive stress tensor (Nikora *et al.* 2001, Poggi *et al.* 2004, Campbell 2005); the last two terms in equation (4) correspond to the form- and viscous-induced drags due to the existence of protruding bed forms. The viscous and Reynolds stress tensors, corresponding to the first two terms within the brackets containing the total stress tensor, appear spatially-averaged in equation (4).

In the present paper we assess experimentally the quantities, $\langle \overline{u_i} \rangle$, $\tilde{u}_i$, $\langle \overline{u'_j u'_i} \rangle$, $\langle \tilde{u}_j \tilde{u}_i \rangle$ and the function Ψ. Given the turbulent nature of the flow, the viscous contribution is negligible. Thus it is not considered in the present study for the estimate of the total stresses tensor.

3 FIELD MEASUREMENTS

3.1 *Flow measurements*

The present measurements were taken during the summer of 2004, in the Swiss river Venoge (canton of Vaud). Fifteen instantaneous velocity profiles were measured in a single day under stationary shallow water flow conditions, as confirmed by the discharge data provided by the Swiss Hydrological and Geological Services. The measuring station was located about 90 m upstream of the Moulin de Lussery. The river hydraulic characteristics at the time of the measurements are shown in Table 1.

Table 1. Summary of the river hydraulic characteristics.

Q	s	h	B	Re	Fr	D_{50}	D_{84}	h/D_{50}
m^3s^{-1}	%	m	m	$(x10^{-4})$	-	mm	mm	(-)
0.76	0.33	0.20	6.30	12	0.43	68	89	2.94

where Q is the discharge; s, the river slope; B, the river width; Re, Reynolds number; Fr, the Froude number; D_{50} and D_{84}, the bed grain size diameter for which 50% and 84% of the grain diameters are respectively smaller. The water depth, h, is the difference of level between the water surface and the lowest trough in the riverbed.

The riverbed material was sampled according to the Wolman method (Wolman 1954), and analyzed using standard sieve sizes to obtain the weighted grain size distribution. The riverbed is hydraulically rough and composed of coarse and randomly spaced gravel. There was no sediment transport during the measurements.

The measurements were made on a 3x5 rectangular horizontal grid. 15 velocity profiles were equally spaced in the spanwise direction by 10 cm and in the streamwise direction by 15 cm. The ideal number of velocity measured profiles to estimate good quality double-averaged quantities is still an open subject although recent developments on the search for optimal measuring conditions indicate that a combination of density and position of profiles has to be satisfied (i.e. Ricardo, 2009). The profiles herein analyzed were obtained on different representative positions of the bed variability and over a window larger than the characteristic wavelength of boundary irregularities (roughly by D_{84}). The vertical resolution of the measurements is about 0.5 cm. The level of the riverbed was determined by the sonar-backscattered response. The profiles were measured for 3.5 min.

3.2 *Instrumentation*

A field deployable ADVP developed at the LHE-EPFL, allows measuring 3D quasi-instantaneous velocity profiles over the entire depth of the river flow. Its resolution permits evaluating the main turbulent flow parameters. The detailed ADVP working principle is given in Rolland and Lemmin (1997). We used a configuration of the ADVP consisting of four receivers and one emitter, which provides one redundancy in the 3D velocity profile measurements. This redundancy is used for noise elimination and data quality control (Hurther and Lemmin 2000, Blanckaert and Lemmin 2006). This configuration combined with a dealiasing algorithm developed by the authors (Franca and Lemmin 2006) theoretically allows noise-free 3D cross-correlation estimates. A Pulse Repetition Frequency (PRF) of 1666 Hz and a Number of Pulse Pairs (NPP) of 64 were used for the estimate of the Doppler shift, thus resulting in a sampling frequency of 26 Hz. A bridge which supported the ADVP instrument allowed the easy displacement of the system across the section and along the river streamwise direction, thus minimizing ADVP vibration and flow disturbance.

3.3 *Void fraction*

The void fraction (Figure 1), or porosity, corresponds to the ratio of the area occupied by the fluid to the area occupied by the solid elements from the bed at a given elevation.

The void fraction, between the troughs and crests of the riverbed, was determined from the detection of local bed elevations obtained with the Doppler echo provided by the ADVP. Above the highest crest, located at $z/h \approx 0.40$, the void fraction corresponds to 1.0, which means that the domain parallel to the riverbed is entirely filled by the fluid. Below the lowest trough, we used a constant value of 0.38 of the void fraction which corresponds to an asymptotic convergence, as has been verified in laboratory tests with similar reconstituted gravel beds.

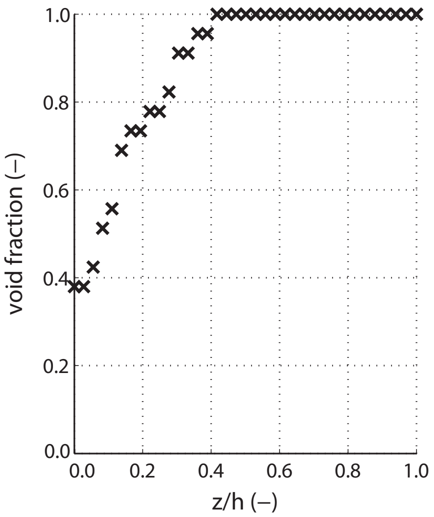

Figure 1. Distribution of the void fraction.

4 RESULTS

4.1 *Double-averaged velocities*

Figures 2 to 4 present, for the streamwise, spanwise and vertical components, the time-averaged and double-averaged velocity profiles, corresponding to, respectively,

Figure 2: $\overline{u}$ and $\left\langle \overline{u} \right\rangle(z) = \dfrac{1}{A_f(z)} \int_\Omega \overline{u}(\alpha,\beta,z)\mathrm{d}S$

Figure 3: $\overline{v}$ and $\left\langle \overline{v} \right\rangle(z) = \dfrac{1}{A_f(z)} \int_\Omega \overline{v}(\alpha,\beta,z)\mathrm{d}S$

Figure 4: $\overline{w}$ and $\left\langle \overline{w} \right\rangle(z) = \dfrac{1}{A_f(z)} \int_\Omega \overline{w}(\alpha,\beta,z)\mathrm{d}S$

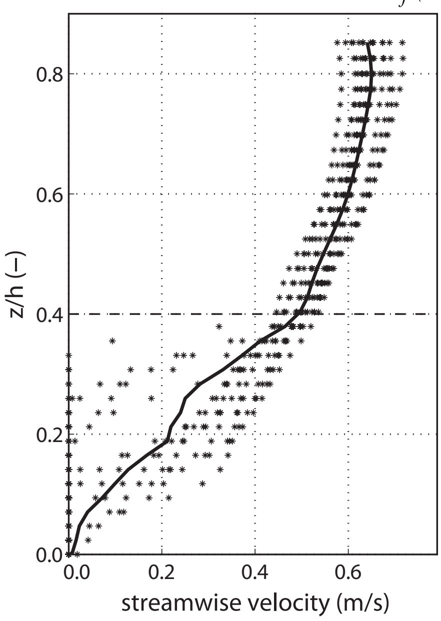

Figure 2. Time-averaged (*) and double-averaged (thick line) streamwise velocity profiles. Time-averaged data (*) correspond to the 15 measured profiles.

From the analysis of the double-averaged streamwise velocity profiles, one may corroborate the findings in Franca *et al*. (2008) where the flow was considered to be divided into the three layers: inner, intermediate and outer. A logarithmic-like distribution exists in the intermediate region and extends roughly from $z/h = 0.40$ to $z/h = 0.80$.

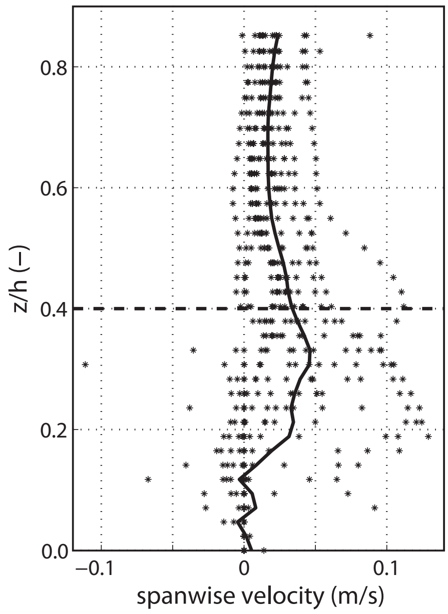

Figure 3. Time-averaged (*) and double-averaged (thick line) spanwise velocity profiles. Time-averaged data (*) correspond to the 15 measured profiles.

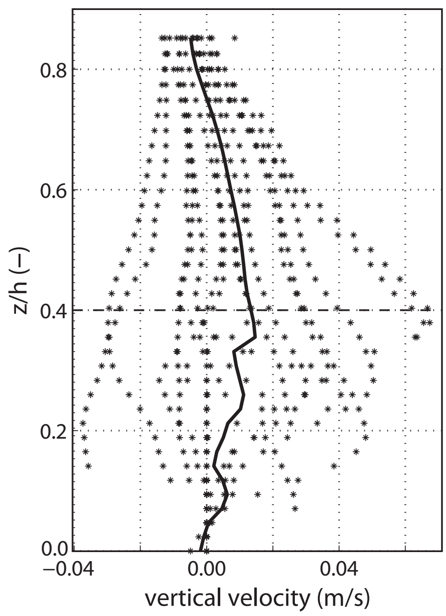

Figure 4. Time-averaged (*) and double-averaged (thick line) vertical velocity profiles. Time-averaged data (*) correspond to the 15 measured profiles.

Below $z/h = 0.40$, roughly between $z/h = 0.30$ and 0.35, a linear region is observed which is in accordance with the findings by the authors in Ferreira *et al*. (2009).

Within the inner layer, $z/h < 0.40$, the double-averaged streamwise velocity profile is inflected as expected between the troughs and crests of the riverbed (Katul *et al*. 2002). The limit $z/h < 0.40$ corresponds roughly to D_{84} of the riverbed grain size distribution; this grain size is considered by several authors as the principal scale for bed protuberances (Bathurst 1988). The inner layer corresponds to the roughness layer, as described by Nikora and Smart (1997) and Smart (1999), where random deviations of time-averaged velocity profiles and three-dimensionality occur. In our study, the flow is mainly conditioned by the bed roughness, and self-similarity of time-averaged quantities does not exist.

The time-averaged velocity profiles confirm the heterogeneity and three-dimensionality of the present flow. The double-averaged profiles are not conclusive and seem to be influenced by a few extreme time-averaged profiles; given the discrepancies between time-averaged profiles, the discussion on spanwise and vertical double-averaged velocity profiles requires additional measurements in the river.

4.2 *Double-averaged fluid stresses*

Figures 5 to 7 present, for the streamwise, spanwise and vertical components, Reynolds, form-induced and total normal stresses per unit mass, corresponding to, respectively,

Figure 5: $-\Psi\left\langle\overline{u'u'}\right\rangle$, $-\Psi\left\langle\tilde{u}\tilde{u}\right\rangle$ and $\frac{1}{\rho}\left\langle\tau_x\right\rangle$

Figure 6: $-\Psi\left\langle\overline{v'v'}\right\rangle$, $-\Psi\left\langle\tilde{v}\tilde{v}\right\rangle$ and $\frac{1}{\rho}\left\langle\tau_y\right\rangle$

Figure 7: $-\Psi\left\langle\overline{w'w'}\right\rangle$, $-\Psi\left\langle\tilde{w}\tilde{w}\right\rangle$ and $\frac{1}{\rho}\left\langle\tau_z\right\rangle$

As mentioned above, the viscous stress is negligible, and therefore not used in the estimate of the total stresses.

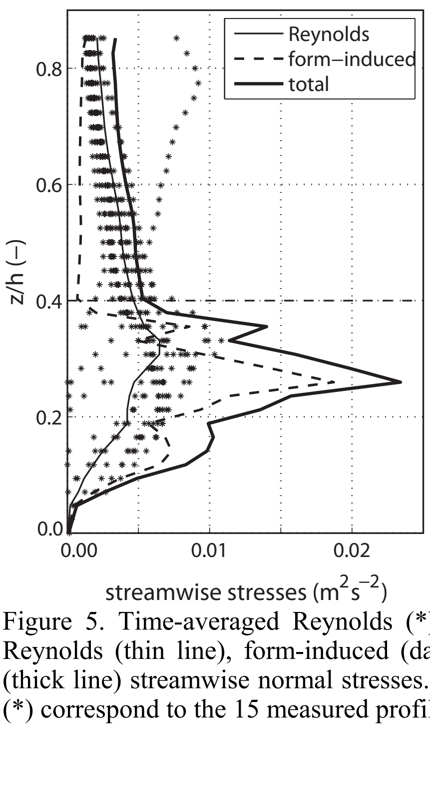

Figure 5. Time-averaged Reynolds (*), spatially-averaged Reynolds (thin line), form-induced (dashed line) and total (thick line) streamwise normal stresses. Time-averaged data (*) correspond to the 15 measured profiles.

Some heterogeneity is found in the amplitude of time-averaged stresses, especially in the vertical component, but they all show similar distribution patterns.

It can be seen from Figures 5 to 7 that form-induced stresses are of the same order of magnitude as Reynolds stresses. In the streamwise case, form-induced stress has three times the value of Reynolds stress. In all three cases, form-induced stresses contribute largely to total stresses, especially below the top of the riverbed crests.

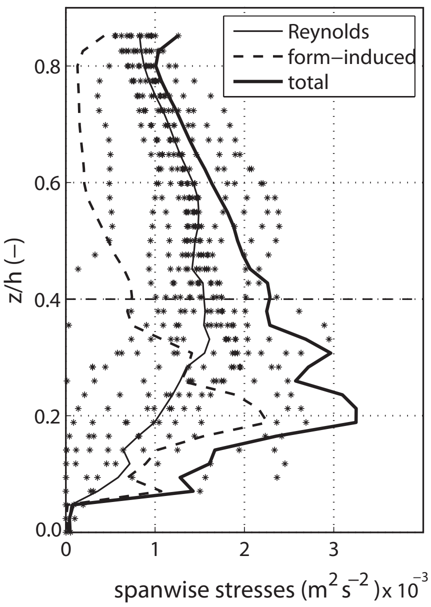

Figure 6 Time-averaged Reynolds (*), spatially-averaged Reynolds (thin line), form-induced (dashed line) and total (thick line) spanwise normal stresses. Time-averaged data (*) correspond to the 15 measured profiles.

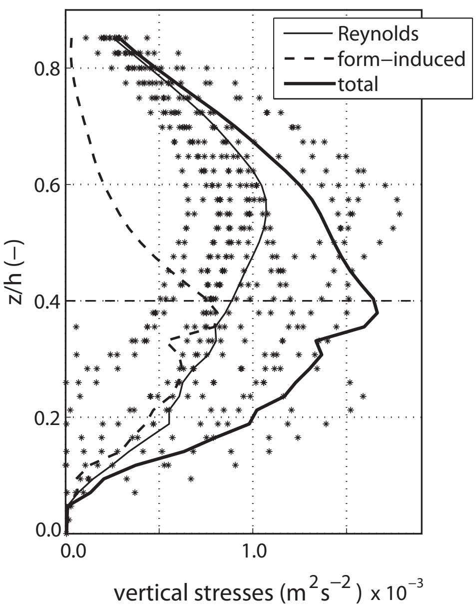

Figure 7. Time-averaged Reynolds (*), spatially-averaged Reynolds (thin line), form-induced (dashed line) and total (thick line) vertical normal stresses. Time-averaged data (*) correspond to the 15 measured profiles.

Streamwise and spanwise Reynolds stresses peak at around $z/h \approx 0.35$, whereas form-induced stresses peak slightly below, at $z/h \approx 0.25$. In both cases the peak value of form-induced stresses are higher than Reynolds peaks, and the total stresses maxima are located at $z/h \approx 0.25$, well between the troughs and crests of the riverbed.

Vertical Reynolds peak stresses are located high in the water column, roughly at $z/h \approx 0.55$. Form-induced and total vertical stresses peak at the level corresponding to the highest crests of the riverbed.

5 DISCUSSION AND CONCLUSIONS

The double-averaging concept was applied to ADVP field measurements which allowed new insight into the turbulence structure of this flow field under low values of relative submergence and into the balance between Reynolds and form-induced stresses.

The roughness layer is well defined and corresponds to the region below the riverbed crests; the upper limit, situated at $z/h \approx 0.40$, corresponds to the D_{84} of the bed material.

Form-induced stresses are important. They are of the same order of magnitude or higher than Reynolds stresses within the roughness layer, and largely condition total stress distribution. Total stresses peak inside the roughness layer, and tend to zero near the lowest troughs of the riverbed.

Further investigation will evaluate the balance between stress and drag in the momentum equation, especially between the troughs and crests of the riverbed.

ACKNOWLEDGEMENTS

The authors wish to acknowledge the financial support by the Swiss National Science Foundation (2000-063818) and by the Portuguese Science and Technology Foundation (PTDC/ECM/65442/2006 and PTDC/ECM/099752/2008).

REFERENCES

Baiamonte, G., Ferro, V. 1997. The influence of roughness geometry and Shields parameter on flow resistance in gravel-bed channels. Earth Surface Processes and Landforms, Vol. 22, 759-772.

Bathurst, J.C. 1988. Velocity profile in high-gradient, boulder-bed channels. Proc. Int. Conf. Fluv. Hydr., Budapest.

Blanckaert, K., Lemmin, U. 2006. Means of noise reduction in acoustic turbulence measurements. J Hydr Res, 44, 3-17.

Buffin-Bélanger, T., Roy, A.G. 1998. Effects of a pebble cluster on the turbulent structure of a depth-limited flow in a gravel-bed river, Geomorphology, Vol. 25, 249-267.

Buffin-Bélanger, T., Roy, A.G. 2005. 1 min in the life of a river: selecting the optimal record length for the measurement of turbulence in fluvial boundary layers. Geomorphology, 68, 77-94

Campbell, L.J. 2005. Double-averaged open-channel flow over regular rough beds. PhD Thesis, Dept. of Engineering - University of Aberdeen. Aberdeen.

Ferreira, R.M.L., Ferreira, L.M., Ricardo, A.M., Franca, M.J. 2009. Impacts of sand transport on flow variables and dissolved oxygen in gravel-bed streams suitable for salmonid spawning. River. Res. Applic, in press.

Finnigan, J.J. 2000. Turbulence in plant canopies. Annual Review of Fluid Mechanics 32, 519–571.

Finnigan, J.J., Shaw, R.H. 2008. Double-averaging methodology and its application to turbulent flow in and above vegetation canopies. Acta Geophysica 56, 534–561.

Franca, M.J., Lemmin, U. 2006. Eliminating velocity aliasing in acoustic Doppler velocity profiler data. Meas Sci Technol, 17, 313-322.

Franca, M.J., Czernuszenko, W. 2006. Equivalent velocity profile for turbulent flows over gravel riverbeds. River Flow 2006, Taylor & Francis Group, London, Vol. 1, 189-198.

Franca, M.J., Ferreira, R.M.L., Lemmin, U. 2008. Parameterization of the logarithmic layer of double-averaged streamwise velocity profiles in gravel-bed river flows. Advances in Water Resources 31, 915–925.

Gimenez-Curto, L.A., Corniero Lera, M.A. 1996. Oscillating turbulent flow over very rough surfaces. J Geophys Res, 101(C9), 20745–20758.

Hinze J.O. Turbulence. McGraw-Hill 1975, New York.

Hurther, D., Lemmin, U. 2000. A correction method for turbulence measurements with a 3D acoustic Doppler velocity profiler. J Atmosph Ocean Technol, 18, 446-458.

Katul, G, Wiberg, P, Albertson, J, Hornberger, G. 2002. A mixing layer theory for flow resistance in shallow streams. Water Resour Res, 38(11), 1250.

Kirkbride, A.D. and Ferguson, R. 1995. Turbulent flow structure in a gravel-bed river: Markov chain analysis of the fluctuating velocity profile, Earth Surf. Proc. and Landforms, 20, 721-733.

Lopez, F., Garcia, M.H. 2001. Mean flow and turbulence structure of open-channel flow through emergent vegetation. J Hydraul Eng, 127(5), 392-402.

Nikora, V., Smart, G.M. 1997. Turbulence characteristics of New Zealand gravel-bed rivers. J Hydr Eng 23(9), 764-773.

Nikora, V.I., Goring, D.G., McEwan, I.K., Griffiths, G. 2001. Spatially averaged open-channel flow over rough bed. J Hydr Eng, 127(2),123-133.

Nikora, V., McEwan, I., McLean, S., Coleman, S., Pokrajac, D., Walters, R. 2007. Double-averaging concepts for rough-bed open-channel and overland flows: Theoretical background. J Hydr Eng 133(8), 873–883.

Poggi, D., Katul, G., Albertson, J. 2004. A note on the contribution of dispersive fluxes to momentum transfer within canopies. Boundary Layer Meteorology 111, 615–621.

Pokrajac, D., McEwan, I., Nikora, V. 2008. Spatially averaged turbulent stress and its partitioning. Exp Fluids 45, 73–83.

Raupach, M.R., Antonia, R.A., Rajagopalan, S. 1991. Rough-wall turbulent boundary layers. Appl. Mech. Rev. 44(1), 1–25.

Ricardo, A.M. 2006. Optimizing the location of sampling points for double-averaged turbulent quantities in flows within arrays of rigid emergent stems. 33rd IAHR Congress, Vancouver.

Rolland, T., Lemmin, U. 1997. A two-component acoustic velocity profiler for use in turbulent open-channel flow. J Hydr Res, 35(4), 545-561.
Smart, G.M. 1999. Turbulent velocity profiles and boundary shear in gravel bed rivers. J Hydr Eng 125(2), 106-116.
Smith, J.D., McLean, S.R. 1977. Spatially averaged flow over a wavy surface. J Geophys Res 83(12), 1735-1746.
White, B. L., Nepf, H. M. 2008. A vortex-based model of velocity and shear stress in a partially vegetated shallow channel. Water Resources Research 44(1), W01412.
Wolman, M.G. 1954. A method of sampling coarse river-bed material, Trans. Amer. Geoph. Un., Vol. 35, 951-956.